

RESEARCH ARTICLE

Open Access



The morphology and metabolic changes of *Actinobacillus pleuropneumoniae* during its growth as a biofilm

QiuHong Zhang^{1,2}, Lu Peng^{1,2}, Weiyao Han^{1,2}, Hongyu Chen^{1,2}, Hao Tang^{1,2}, Xiabing Chen³, Paul R. Langford⁴, Qi Huang^{1,2,5}, Rui Zhou^{1,2,5} and Lu Li^{1,2,5*} 

Abstract

Actinobacillus pleuropneumoniae is an important swine respiratory pathogen. Previous studies have suggested that growth as a biofilm is a natural state of *A. pleuropneumoniae* infection. To understand the survival features involved in the biofilm state, the growth features, morphology and gene expression profiles of planktonic and biofilm *A. pleuropneumoniae* were compared. *A. pleuropneumoniae* in biofilms showed reduced viability but maintained the presence of extracellular polymeric substances (EPS) after late log-phase. Under the microscope, bacteria in biofilms formed dense aggregated structures that were connected by abundant EPS, with reduced condensed chromatin. By construction of Δpga and $\Delta dspB$ mutants, polymeric β -1,6-linked N-acetylglucosamine and dispersin B were confirmed to be critical for normal biofilm formation. RNA-seq analysis indicated that, compared to their planktonic counterparts, *A. pleuropneumoniae* in biofilms had an extensively altered transcriptome. Carbohydrate metabolism, energy metabolism and translation were significantly repressed, while fermentation and genes contributing to EPS synthesis and translocation were up-regulated. The regulators Fnr (HlyX) and Fis were found to be up-regulated and their binding motifs were identified in the majority of the differentially expressed genes, suggesting their coordinated global role in regulating biofilm metabolism. By comparing the transcriptome of wild-type biofilm and Δpga , the utilization of oligosaccharides, iron and sulfur and fermentation were found to be important in adhesion and aggregation during biofilm formation. Additionally, when used as inocula, biofilm bacteria showed reduced virulence in mouse, compared with planktonic grown cells. Thus, these results have identified new facets of *A. pleuropneumoniae* biofilm maintenance and regulation.

Keywords *Actinobacillus pleuropneumoniae*, biofilm, planktonic, morphology, transcription, metabolism, regulator

Handling editor: Marcelo Gottschalk

*Correspondence:

Lu Li
lilu@mail.hzau.edu.cn

¹ National Key Laboratory of Agricultural Microbiology, College of Veterinary Medicine, Huazhong Agricultural University, Wuhan 430070, Hubei, China

² Key Laboratory of Preventive Veterinary Medicine in Hubei Province, The Cooperative Innovation Center for Sustainable Pig Production, Wuhan 430070, Hubei, China

³ Institute of Animal Husbandry and Veterinary Science, Wuhan Academy of Agricultural Sciences, Wuhan 430070, Hubei, China

⁴ Section of Paediatric Infectious Disease, Imperial College London, St Mary's Campus, London W2 1PG, UK

⁵ International Research Center for Animal Disease, Ministry of Science and Technology of the People's Republic of China, Wuhan 430070, Hubei, China



© The Author(s) 2023. **Open Access** This article is licensed under a Creative Commons Attribution 4.0 International License, which permits use, sharing, adaptation, distribution and reproduction in any medium or format, as long as you give appropriate credit to the original author(s) and the source, provide a link to the Creative Commons licence, and indicate if changes were made. The images or other third party material in this article are included in the article's Creative Commons licence, unless indicated otherwise in a credit line to the material. If material is not included in the article's Creative Commons licence and your intended use is not permitted by statutory regulation or exceeds the permitted use, you will need to obtain permission directly from the copyright holder. To view a copy of this licence, visit <http://creativecommons.org/licenses/by/4.0/>. The Creative Commons Public Domain Dedication waiver (<http://creativecommons.org/publicdomain/zero/1.0/>) applies to the data made available in this article, unless otherwise stated in a credit line to the data.

Introduction

Biofilms are compacted and functionally coordinated aggregates of bacterial cells attached to or embedded on biotic or abiotic surfaces, and their metabolic state, pathogenicity and immunogenicity are different from those of bacteria in the planktonic state [1, 2]. Biofilms contain extracellular polymeric substances (EPS) comprising cross-linked polysaccharides, proteins and/or extracellular DNA, which form a solid physical barrier enabling defense against external environmental stresses [3]. EPS can also mask antigenic epitopes on bacterial surfaces [4]. Bacteria in biofilms can release extracellular nucleases to degrade neutrophil extracellular traps (NETs) [5]. Such features result in biofilms inducing a lower host inflammatory response compared with their planktonic counterparts, and facilitate immune escape [6]. Bacteria inside the biofilm initiate the stringent response, enter dormancy, express efflux pumps and transfer drug-resistant genes horizontally, all of which contribute to resistance against adverse stressors [7]. Hence, the biofilm mode of growth is often associated with persistent infection and acts as a reservoir for recurrent infection.

Biofilm formation depends on the host environment and is regulated by many bacterial signal transduction systems including quorum sensing, two-component, secondary messenger transduction and stringent response systems [8–10]. In *Staphylococcus aureus*, the Agr quorum sensing (QS) system coordinates with multiple global regulatory factors including SarA, CcpA, Fur and two-component systems including SaeRS and LytSR to regulate the production of extracellular DNA, lectin and bacterial surface proteins, all of which are the main components of biofilm EPS [10, 11]. The secondary messenger molecule C-di-GMP is also a known key factor of bacteria involved in biofilm formation [12]. In *Pseudomonas aeruginosa* and *Escherichia coli*, C-di-GMP regulates the production of extracellular polysaccharides and cellulose [13].

Actinobacillus pleuropneumoniae is an important respiratory pathogen of swine, which has high lethality rate resulting in significant economic losses in the world swine industry [14]. In addition to acute infection, *A. pleuropneumoniae* can persist in the tonsils and lungs of sub-clinically infected pigs, becoming a potential source of disease outbreaks [15, 16]. It has been reported that most field isolates of *A. pleuropneumoniae* can form biofilms [17], and pigs naturally infected with the bacterium can be present as biofilm aggregates in the lungs [18]. A recent study found a negative correlation between the ability of field isolates of *A. pleuropneumoniae* to form biofilms in vitro and the severity of pig lung pathological injury [17]. Additionally, it has also been reported that *A. pleuropneumoniae* present in swine farm environmental

samples show strong biofilm formation in vitro [19], and the bacterium can use products of other bacteria to enable its growth in mixed biofilms [20, 21]. *A. pleuropneumoniae* growing in the biofilm mode of growth has enhanced antibiotic resistance [22], and a low propensity to stimulate the immune system because of lipid A modification [23]. Therefore, growth in biofilms is considered a natural state of *A. pleuropneumoniae* during persistent infection [21]. Understanding the structure and survival mechanisms of *A. pleuropneumoniae* in biofilms is crucial for developing methods of prevention and elimination.

The regulation and formation of *A. pleuropneumoniae* biofilms is a complex process. Previous studies have shown that poly-beta (1,6)-N-acetyl-d-glucosamine (PNAG), synthesized and exported by proteins encoded by the *pgaABCD* locus, is a major polysaccharide component of the EPS of some Gram-negative bacteria including *A. pleuropneumoniae* [24]. *A. pleuropneumoniae* also possesses the gene encoding dispersin B (*dspB*) which is a glycosidase that degrades PNAG [25]. The histone-like nucleoid structuring protein H-NS and sigma E directly represses and activates the expression of *pga*, respectively [26]. Many other genes have been found to directly or indirectly affect *A. pleuropneumoniae* biofilm formation, including those encoding the type 2 quorum sensing signal synthetic enzyme LuxS, the two-component signaling systems (TCS) ArcAB and CpxAR, and the stringent response system [27–32]. The transcriptomes of static and biofilms at different growth stages in a drip-flow apparatus have also been compared [33]. Generally, genes involved in energy metabolism were down-regulated, while genes encoding some transporters were up-regulated in biofilms, compared with the planktonic counterparts. The study [33] used microarray hybridization, a technique that has now been superseded by RNA-seq.

To further understand the survival and regulation mechanisms of *A. pleuropneumoniae* growing as a biofilm, in this study, we compared the growth features, morphologies, gene expression profiles (using RNA-Seq) and virulence in mice of planktonic and biofilm grown bacteria. Significant differences in growth, morphology, transcriptome and virulence were found, and three major regulators (Fnr/HlyX and Fis) were identified as being important for the biofilm mode of growth. Our results deepen the understanding of the *A. pleuropneumoniae* biofilm mode of growth.

Materials and methods

Bacterial strains and growth conditions

The strains, plasmids and primers used in this study are listed in Additional file 3. All *A. pleuropneumoniae* strains were cultured at 37 °C on TSA plates or in TSB

medium (Becton, Dickinson and Company, NJ, USA) supplemented with 10 µg/mL NAD. Chloramphenicol at 2 µg/mL was added into the medium when screening for *A. pleuropneumoniae* mutants or complementary strains containing recombinant plasmid. All *E. coli* strains were cultured at 37 °C on LA plate or in LB medium (OXOID, Hampshire, UK). *E. coli* DH5α, TOP10 and β2155 containing recombinant plasmids were screened on LA plates containing 20 µg/mL chloramphenicol. An additional 50 µg/mL 2,6-diaminoheptanoic acid (DAP, Sigma-Aldrich, Darmstadt, Germany) supplementation was required for the cultivation of strain β2155.

Culture and detection of growth feature of planktonic bacteria

For each *A. pleuropneumoniae* culture replicate, a single colony of the bacteria on TSA plate kept in 4 °C less than 4 days was incubated into TSB medium overnight (12–14 h) by shaking at 180 r/min at 37 °C. For culture of *A. pleuropneumoniae* planktonic bacteria (PK), overnight-cultures were transferred to 5 mL fresh TSB medium at 1:100 and cultured at 37 °C at 180 r/min. Samples of planktonic bacteria were taken at 0, 2.5, 4, 5.5, 8, 12 and 24 h. At each timepoint, the OD_{600nm} of the culture was measured and bacterial numbers were determined by viable bacterial counts by plating the cultures onto TSA plates after serial dilutions in normal saline from 10⁻³ to 10⁻⁶. Three plating replicates were conducted for each dilution. After incubation of the plates at 37 °C overnight, the colony forming units (CFU) on each plate were recorded and the original bacterial numbers in each group were calculated.

Culture and detection of growth feature of biofilm

For culture of biofilm (BF), overnight-cultures of *A. pleuropneumoniae* were transferred into BHI (OXOID, Hampshire, UK) [8] at 1:75 in 12-wells flat bottom cell culture plates (LabServ; Thermo Fisher Scientific, Shanghai, China) at 2 mL per well and incubated at 37 °C statically. Samples were collected at 0, 2.5, 4, 5.5, 8, 12 and 24 h for bacterial numbers measurement and crystal violet (CV) staining of biofilm. The upper suspension was separated and diluted in normal saline for determination of bacterial numbers. The adhesion layer bacteria were collected as biofilms and resuspended in 2 mL of saline, dispersed totally by vortex and diluted in saline. The bacterial numbers in the dilutions were determined by viable bacterial counts as described above.

For quantifications of the biomass of the adherent layer, the upper suspensions were discarded and the wells were gently washed twice with normal saline to remove unattached bacteria and residual medium, followed by fixation of the adherent layer after air-dry. Then, 2 mL

of 0.1% Crystal Violet Ammonium Oxalate Solution (Beijing Solarbio Science & Technology Co., Ltd. China) was added into each well to stain the fixed biofilm layer, which was incubated at 37 °C for 15 min. After washing the wells with saline, the dyed adherent layers were dissolved by 2 mL of 33% glacial acetic acid solution per well and resuspended by pipetting. The OD_{595nm} of the dissolved solutions in the wells were measured.

Construction of mutants and complementary strains

The mutants Δ*pgaABCD* and Δ*dspB* were constructed according to the methods described in our previous studies [34]. Briefly, using *A. pleuropneumoniae* 4074 genome as template, upstream and downstream fragments of *pgaABCD* and *dspB* were amplified with primers *pga1/2-pga3/4* and *dspB1/2-dspB3/4*, respectively (Additional file 3). The amplified products were ligated to the Sall/NotI site of pEMOC2 [35] using the ClonExpress MultiS One Step Cloning Kit (Nanjing Vazyme Biotech Co., Ltd., China). Then the recombinant plasmid was transformed from *E. coli* β2155 to *A. pleuropneumoniae* WT strain by conjugation [35]. The suspected mutants were screened using the plates supplemented with 2 µg/mL chloramphenicol and 10% (v/w) sucrose and mutants confirmed by PCR using the primers in Additional file 3.

The complementary strains were constructed using the plasmid pMC-express [36] (Additional file 3). The full-length fragments of *pgaABCD* and *dspB* were amplified with primers pMC-*pga* F/R and pMC-*dspB* F/R, respectively, using *A. pleuropneumoniae* 4074 genome as template (Additional file 3). The amplification products were cloned into pMC-express vector cut with KpnI and NotI. The recombinant plasmid was transformed into the corresponding mutant strains by electroporation. The transformants were screened using the plates with chloramphenicol (2 µg/mL) and the complementary strains were confirmed by PCR using the primers in Additional file 3.

Morphological observations

The planktonic and biofilm grown bacteria were cultured to logarithmic phase as described above and observed under a transmission electron microscope (TEM) and a scanning electron microscope (SEM). Planktonic or bacteria obtained from the biofilm adhesion layer were centrifuged at 5000 g for 5 min and fixed in 2.5% glutaraldehyde. For observation under TEM, the fixed cells were rinsed for 15 min in 0.1 M phosphate buffer (pH 7.4) 3 times. The cells were further fixed with 1% osmic acid-0.1 M phosphate buffer (pH 7.4) at room temperature for 2 h and rinsed with 0.1 M phosphate buffer (pH 7.2) 3 times. The samples were dehydrated by an alcohol gradient (30%, 50%, 70%, 80%, 90%, 95%, 100%) and

permeated by epoxy (2:1), acetone: epoxy (1:1) and epoxy. The epoxy was embedded and sectioned, and then double-stained with uranium and the bacterial morphologies were observed under TEM (Tecnai G20 TWIN, FEI, USA).

For observation under SEM, the immobilized bacterial samples were washed with PBS (0.1 M, no NaCl) 3–5 times. After gradient dehydration with alcohol, the samples were treated with isoamyl acetate 3 times each for 20 min. The dehydrated samples were dried and sprayed in vacuum. Finally, the morphology of bacteria was observed using high-resolution SEM (Hitachi U8010, Hitachi, Ltd., Japan).

RNA extraction and transcriptome analysis

After overnight culture, the WT planktonic bacteria were sub-cultured for 4 h to log-phase. WT and Δpga were sub-cultured in 12-well plates at 37 °C for 5 h (log-phase). WT biofilms were sampled from the adherent layer. Since Δpga does not form any adherent layer, the whole cultures of this strain were sampled. Then, the planktonic and biofilm grown cells were collected by centrifugation at 5000 g, and total RNA extracted using the Total RNA Extraction Kit (Tianmo Biotech, Beijing, China) according to the protocol recommended by the manufacturer. Each group of samples had three independent biological replicates.

After rRNA removal and quality control, the RNA samples were sequenced. Paired-end sequencing was performed on the Illumina sequencing platform and data quality assessment and filtering was performed by FASTQC and Trimmomatic software. The high-quality sequences obtained after quality control were mapped to the *A. pleuropneumoniae* 4074 genome (NZ_CP029003.1) based on the Burrows-Wheeler method. The RPKM (Reads per Kilobase per Million Reads) value was used as the index of gene expression. The genes with fold change ≥ 2 and p adjust ≤ 0.05 were regarded as differentially expressed genes. Hierarchical clustering was used to classify genes with different expression regulation patterns. Pathway analysis was performed by KEGG pathway enrichment of differentially expressed genes (p value ≤ 0.05).

Quantitative real-time RT-PCR

Culture and RNA extraction of bacteria were described above. Residual gDNA was digested and cDNA was synthesized using the HiScript II 1st Strand cDNA Synthesis Kit (+gDNA wiper; Nanjing Vazyme Biotech Co., Ltd., China). Using the obtained cDNA as template, qPCR was performed with TB Green Premix Ex Taq II Kit (Tli RNaseH Plus) (Takara Biomedical Technology (Beijing) Co., Ltd., China) using primers of differentially

expressed genes listed in Additional file 3. The $2^{-\Delta\Delta Ct}$ of each gene was calculated as the relative expression level with the 16S rRNA expression amount as the endogenous reference.

Mouse infection assay

A model of intranasal infection in mice was used to compare the virulence of *A. pleuropneumoniae* planktonic with biofilm bacteria as described in a previous study [34]. PK and BF bacterial solutions for infection were prepared from log-phase culture as described above. Four-week-old female Kunming mice were anesthetized with 20 μ L/g of Avertin (1.25% tribromoethanol) and intranasally infected with 20 μ L inoculum containing 4×10^6 CFU biofilm ($n=6$) or the same dose of planktonic bacteria ($n=6$), and number of mice surviving recorded for 72 h. For detection of the bacterial loads in the lungs after sub-lethal dose infection of biofilm ($n=6$) or planktonic bacteria ($n=6$), mice were infected intranasally with bacterial cultures from mid-log phase at a dose of 2×10^6 CFU. Then, mice were euthanized at 12, 48 and 72 h after infection. The lungs were collected and thoroughly homogenized and plated on TSA plates after dilution, and the CFUs determined.

Sequence analysis of potential binding sites of regulators

For binding site analysis of differential gene promoter regions, the reference binding motifs of Fnr and Fis were extracted from DB database. The MEME-FIMO online tool (Find Individual Motif Occurrences, p -value < 0.001) was used to search the promoter regions of selected genes for the specific binding motifs of Fnr, Fis and H-NS.

Statistical analysis

A two-tailed t-test was used for statistical analysis of biofilm quantification. The log rank (Mantel-Cox) test was performed for comparison of mortalities of mice in the infection assay. Bacterial loads in the lungs of mice were statistically analyzed using the Mann–Whitney test. Differences with $p < 0.05$ were considered to be significant. For RNA-seq and pathway analysis, the statistical methods have been described above.

Results

A. pleuropneumoniae biofilm differs from planktonic bacteria in their growth curves

A. pleuropneumoniae planktonic or biofilm growth were determined by detecting OD_{600nm} and colony-forming units (CFU) (Figures 1A, B). Bacteria growing in shaking culture or statically in microtiter plates were the source of planktonic and biofilm cells, respectively. For biofilm grown bacteria, CFUs of adherent and non-adherent (upper layer) were determined. Biomass

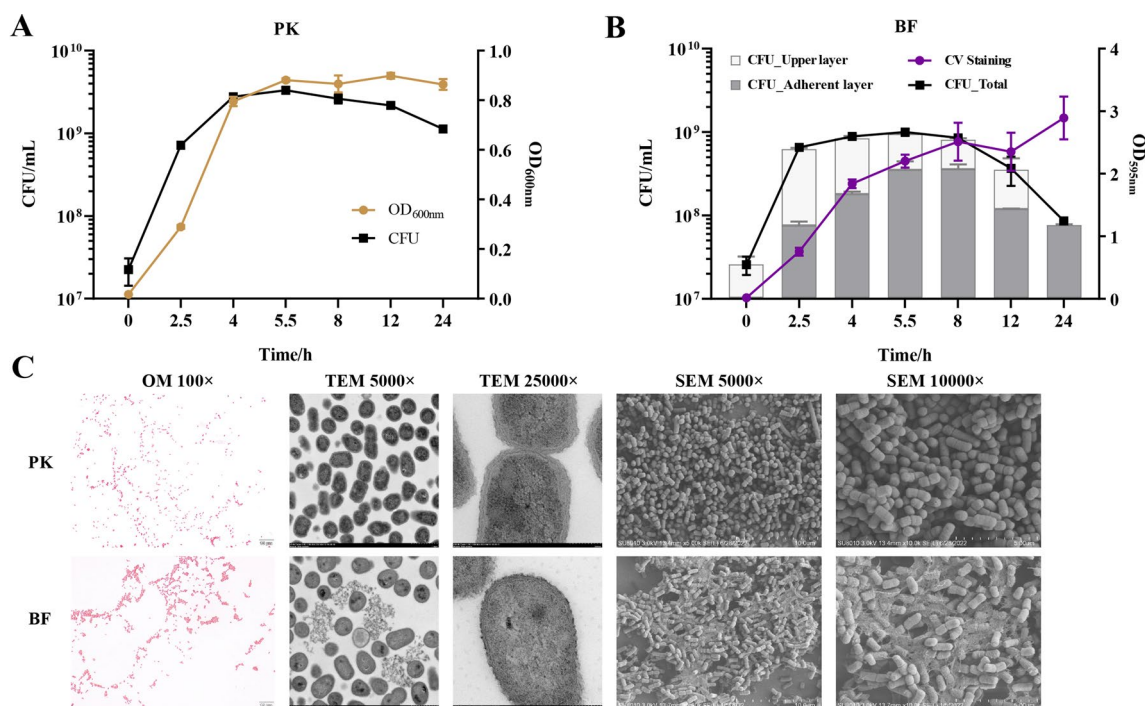


Figure 1 Growth curve and morphological structures of *A. pleuropneumoniae* biofilm and planktonic bacteria. **A** Growth curves represented by bacterial culture absorbance at OD_{600nm} and colony forming units (CFU) of *A. pleuropneumoniae* planktonic bacteria (PK) with shaking at 37 °C. **B** Growth curves of biofilm cells (BF) shown by CFU of the upper and adhesion layers of the biofilm cultures grown statically in 12-well plates (bar graphs). The total CFU of both upper and adhesion layers of the biofilm is shown (black line). Biomass of the biofilms were determined by crystal violet (CV) staining of the adhesion layer (purple line). **C** Morphology of PK and BF grown cells under an optical microscope (OM; Gram staining), transmission electron microscope (TEM) and scanning electron microscope (SEM). The magnification of the image is shown. For growth curves and CV staining of biofilms, data are shown as means ± SD from three independent replicates.

was also quantified by crystal violet (CV) staining. In the early stage of culture (5–6 h), the growth trends of planktonic bacteria and biofilm were similar (Figures 1A, B). Thereafter, as the biofilm approached maturity, planktonic bacteria entered the stationary phase with the highest CFU (Figures 1A, B). The biomass detected by CV staining increased in the early stage of biofilm formation (2.5–5.5 h), which was consistent with the trend of bacterial proliferation as detected by the CFU in both upper and adherent layers (Figure 1B). As the biofilm matured, the quantities of viable bacterial numbers reached its peak at 5.5–8 h, corresponding with the thickest EPS of the biofilm according to the CV staining (Figure 1B). At the later stage of biofilm formation, the quantities of the biomass were stable until 24 h, but the number of viable bacteria in the biofilm layer and upper layer decreased (Figure 1B). Taken together, under the conditions used in this study, the biofilm growth of *A. pleuropneumoniae* entered maturation at 5–5.5 h, the same time as that of late-log phase and the beginning of the stationary

phase of planktonic bacteria. Thereafter, the biomass of biofilm was maintained to 24 h, but the number of viable bacteria declined, while the viable bacteria in planktonic cultures was maintained to 24 h.

Morphological structure of *A. pleuropneumoniae* biofilms

The morphologies of biofilms in the mature stage (5 h) were observed. Gram staining showed that, compared with planktonic bacteria, those grown as biofilm aggregated into clusters with flocculent impurities that could be stained around the clusters (Figure 1C). Transmission electron microscopy revealed that, compared to planktonic bacteria, there were numerous interconnected extracellular flocs in biofilm grown bacteria (Figure 1C), inside of which condensed chromatin could be seen as black clumps or filaments. Compared with planktonic bacteria, there were fewer black masses inside the biofilm (Figure 1C). In mature biofilms observed under scanning electron microscopy, there were dense aggregated structures connected by abundant EPS (Figure 1C).

PNAG and dispersin B are critical for *A. pleuropneumoniae* normal biofilm formation

It has been reported that PNAG and dispersin B are essential for the formation and degradation of *A. pleuropneumoniae* biofilm extracellular matrix [25]. To verify the role of PNAG in biofilm formation and the role of dispersin B in biofilm dispersion of *A. pleuropneumoniae*, we constructed the deletion mutants and complementary strains of *pgaABCD* and *dspB*, respectively (Additional file 1). Deletion of *pgaABCD* (Δpga) and *dspB* ($\Delta dspB$) did not affect *A. pleuropneumoniae* growth (Additional file 2). Gram-staining and electron microscopy indicated that Δpga failed to adhere to microplate surfaces/slide to form a biofilm structure (Figure 2). The results confirmed that PNAG was essential for the formation of a biofilm. In contrast, $\Delta dspB$ exhibited obvious enhanced biofilm formation, with more aggregates and extracellular matrix (Figure 2). Therefore, the above results confirmed that *A. pleuropneumoniae* formed biofilm dependent on PNAG as the main component of the EPS, while dispersin B was involved in limiting biofilm formation.

***A. pleuropneumoniae* grown in biofilms have significantly altered gene transcriptional patterns from planktonic bacteria**

Planktonic wild-type (WT) bacteria were grown to mid-log phase, and WT and Δpga were also grown statically in microplates until the biofilm maturity stage (5 h). The biofilm/adhesion layer of WT (BF), Δpga (unable to generate adhesion layer), and planktonic WT (PK) were harvested for RNA sequencing and analysis. According to the hierarchical clustering heatmap (Figure 3A) and principal component analysis (Figure 3B), there was good reproducibility among the three independent samples in each group. The PK and BF groups had different hierarchical clustering patterns (Figure 3A) and great distance on the x-axis (Figure 3B), indicating that the transcriptional patterns of bacteria grown in biofilms were significantly different to those grown planktonically. Compared with the PK group, there were 646 differentially expressed genes (332 up-regulated, 314 down-regulated) in the BF group (Additional file 4). Generally, the transcriptional pattern of the Δpga group was more similar with that of BF group (Figures 3A, B, Additional file 5), with fewer differentially expressed genes (198 up-regulated, 15 down-regulated).

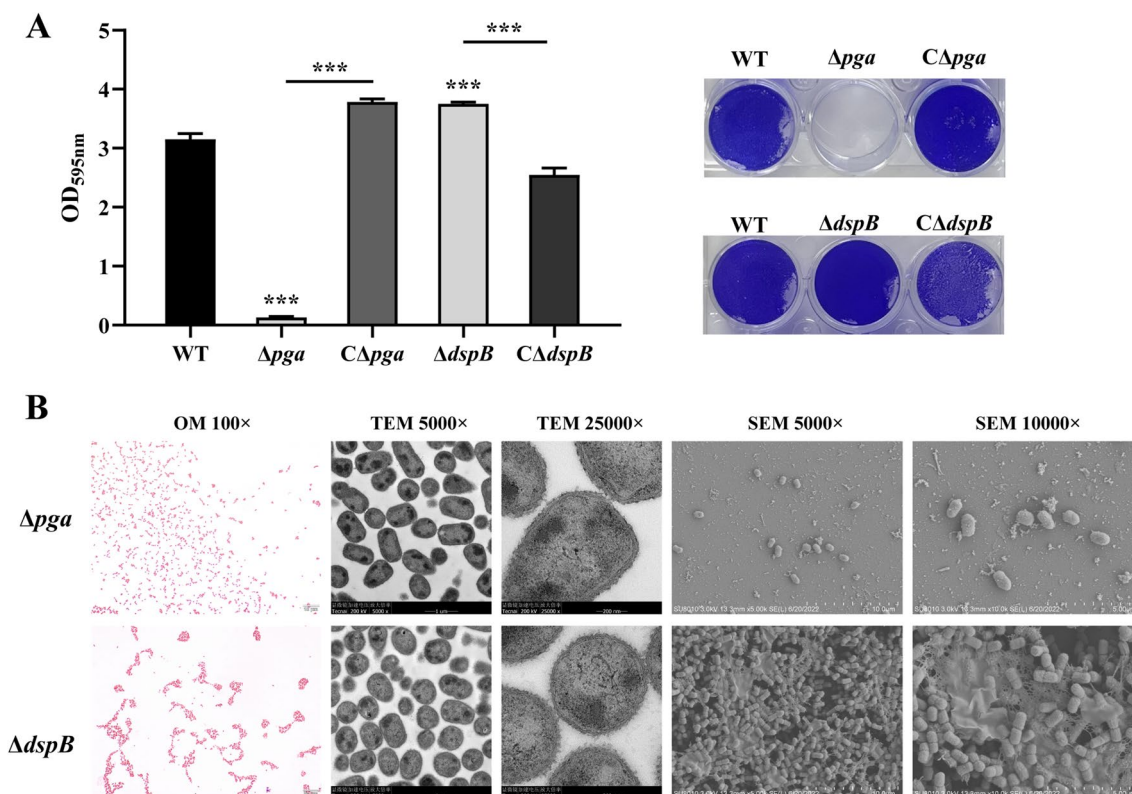


Figure 2 Morphology of Δpga and $\Delta dspB$. **A** CV staining of biofilms formed by WT, Δpga and $\Delta dspB$ cultured for 5 h in 12-well plates. Data are shown as means \pm SD from three independent replicates. A two-tailed t-test was used to compare the biofilm quantities of WT and the Δpga or $\Delta dspB$ (***, $p < 0.001$). **B** Morphology of Δpga and $\Delta dspB$ under optical microscopy (OM; Gram staining), transmission electron microscope (TEM) and scanning electron microscope (SEM). The magnifications of the images are shown

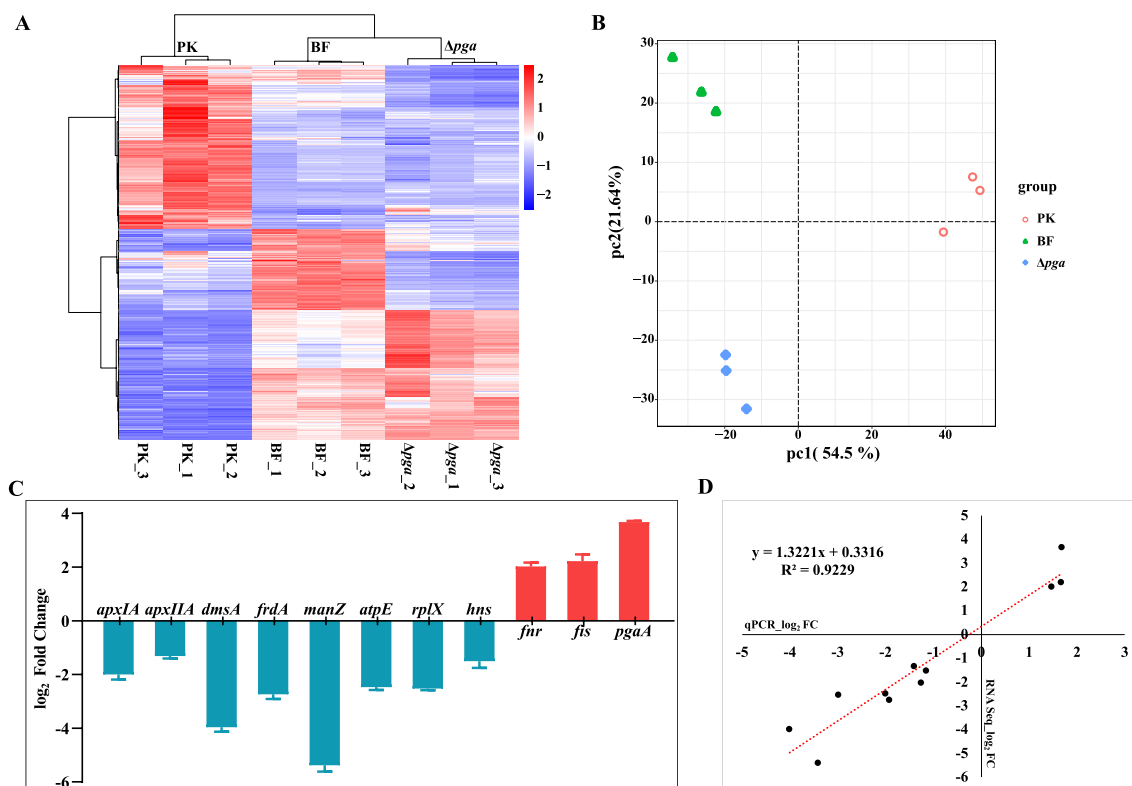


Figure 3 Transcriptome levels and gene expression difference analysis of PK, BF and Δpga . **A** Heatmap of differentially expressed genes from all comparison groups (PK, BF and Δpga) after RNA-seq analysis. The horizontal line represents genes, while each column represents a sample. Each treatment group consisted of three independent biological replicates. Red: genes with increased expression levels. Blue: genes with decreased expression levels. **B** Principal component analysis of gene expressions from all comparison groups (PK, BF and Δpga) after RNA-seq analysis. Different colors represent different groups. **C** The \log_2 fold change values of qRT-PCR showing the transcriptional changes of 11 differentially expressed genes in BF compared with PK group from RNA-seq analysis. **D** Pearson coefficient correlation analysis between qRT-PCR and RNA-seq analysis. X-axis: \log_2 value from qRT-PCR; Y-axis: \log_2 value from RNA-seq.

Transcript levels of 11 genes were determined by qRT-PCR under the same sampling conditions as RNA-Seq (Figure 3C) and correlated well with transcriptome data (Figure 3D).

The transcriptional levels of genes in multiple metabolic pathways of *A. pleuropneumoniae* grown in biofilms were significantly changed

KEGG pathway enrichment analysis was performed on genes differentially expressed in the BF group compared with the PK group, and 124 up-regulated and 201 down-regulated genes were matched into multiple pathways (Figure 4). Among them, the genes involved in metabolism, genetic information and environmental information processing pathways accounted for 45.5%, 23.4% and 16.0% of the total, respectively. Genes involved in carbohydrate metabolism (19.9%), energy metabolism (17.9%), translation (23.4%) and membrane transport (11.4%) accounted for 72.6% (146/201) of the down-regulated, but only 32.3% (40/124) of the up-regulated

genes (Figure 4A). Significantly down-regulated pathways that were enriched included oxidative phosphorylation, phosphotransferase system (PTS), glycolysis/gluconeogenesis, pyruvate metabolism, citrate cycle (TCA cycle), and ribosome synthesis (Figures 4B, 5). ATP synthase and pathways involved in aerobic respiration were significantly down-regulated. Similarly, reduction pathways such as nitrate, TMAO\DMSO and fumaric acid reductions involved in the electron transport chain of anaerobic respiration were also significantly down-regulated (Figure 5). In contrast, the fermentation pathways for lactic acid and ethanol production were up-regulated (Figure 5). The riboflavin metabolic pathway, with its product flavin mononucleotide (FMN) as a cofactor of L-lactate dehydrogenase LldD and various enzymes [37], was up-regulated (Figure 5). The catabolism of stored carbon sources, starch glycogen and N-acetylneuraminic acid (Neu5Ac), were up-regulated. Notably, three enzymes (Nan A/K/E) leading to the production of GlcNAc-6P, the precursor for synthesis of PNAG, peptidoglycan and lipid

A [38–40], were up-regulated. As expected, the *pgaABCD* operon encoding the PNAG synthetase and export proteins was significantly up-regulated (Figure 5). In addition, up-regulated genes involved in other pathways were enriched, for example many genes involved in sulfur metabolism, which is critical for providing sulfur atoms for methionine, glutathione and iron-sulfur clusters (Figure 5). Molybdenum cofactor and folate synthesis, histidine metabolism and some transporters of Fe (III) and Fe (II) were also up-regulated. Altogether, the transcriptional changes of many metabolic genes indicated that bacteria grown in biofilms significantly reduced energy metabolism and genetic activities, increased fermentation and related cofactor synthesis, and accumulated extracellular matrix PNAG.

Analysis of transcriptional regulation in biofilm grown *A. pleuropneumoniae*

As previously described, the formation of a bacterial biofilm and its maintenance requires signal transduction systems and regulators in response to specific conditions or stimuli. We next focused on the differentially expressed transcriptional regulators in *A. pleuropneumoniae* grown in biofilms. In particular, the global regulatory proteins Fnr (also named as HlyX) which is important for the transition from aerobic to anaerobic growth, the nucleoid associated protein Fis, and the histone-like nucleoid associated protein H-NS, were differentially expressed in the biofilm transcriptome.

Fnr is a known global regulator in response to oxygen levels [41]. It was up-regulated in *A. pleuropneumoniae* grown as a biofilm ($\log_2FC=1.470$, Figure 3). Fnr of *A. pleuropneumoniae* consists of 255 amino acids, which is homologous to Fnr of *E. coli* with 75% sequence identity and also with a similar function [42]. The DNA binding motif of Fnr in the upstream region of differentially expressed genes or operons of BF were searched (Additional file 4). The results showed that 63% of these genes had Fnr binding site(s) (Table 1 and Additional file 4, $p<0.001$). Among these genes, most of which were down-regulated, were those involved in transcription and translation, glycolysis, the TCA cycle and anaerobic respiratory electron transport chain. The up-regulated genes mainly participated in L-lactate fermentation, cofactor synthesis (FMN, molybdopterin), amino acid metabolism, Neu5Ac metabolism, PNAG synthesis, and *fnr* itself. Notably, Fnr binding sites were also found in the promoter regions of *apxICABD* and *apxIICA* encoding the important virulence factors of *A. pleuropneumoniae*, the RTX toxins [43]. These genes were also significantly down-regulated when *A. pleuropneumoniae* was growing as a biofilm.

As a multifunctional protein involved in regulation of transcription, replication and recombination, Fis is considered to be an important regulator controlling the transition from log phase to stationary phase during growth [44, 45] and was significantly up-regulated in *A. pleuropneumoniae* biofilms ($\log_2FC=1.672$, Figure 3). Fis of *A. pleuropneumoniae* had 71% sequence identity with that of *E. coli*, with a conserved DNA binding domain at the C-terminus. The Fis binding motif was found in the upstream sequences of 68% of the differentially expressed genes of the BF group (Table 2 and Additional file 4, $p<0.001$). The down-regulated genes with a Fis binding motif in the upstream region were involved in transcription and translation, glycolysis, the TCA cycle, multiple terminal respiratory enzymes and also included *apxIICA*. The up-regulated genes were involved in fermentation, FMN metabolism and folate biosynthesis. Among these genes potentially regulated by Fis, 77.5% contained Fnr binding motifs in their promoters, indicating that these genes were cross-regulated by Fnr and Fis in *A. pleuropneumoniae* biofilms (Table 2). In addition, Fis and HlyX were found to have binding sites of each other in their promoter regions (Table 2).

The known *A. pleuropneumoniae* biofilm regulatory protein H-NS [26] was down-regulated in the biofilm transcriptome ($\log_2FC=-1.158$, Figure 3). H-NS binding sites were found in the upstream regions of 20.7% differentially expressed genes of the BF group (Table 3 and Additional file 4, $p<0.001$), i.e., less than that with Fnr and Fis binding motifs.

Genes associated with bacterial aggregation and adhesion during biofilm formation

Using the transcriptome of Δpga which cannot adhere and form biofilms as the control, the genes differentially expressed in BF were considered as being associated with bacterial aggregation and adhesion during biofilm formation. Among these genes, 198 were up-regulated and 15 were down-regulated, with more than 64% of the genes involved in metabolism. The up-regulated genes included those taking part in metabolism and transport of galactose, mannose, maltose, fucose and Neu5Ac (Table 4 and Additional file 5). These oligosaccharides usually form or modify cell membrane glycoconjugates such as glycoproteins and lipopolysaccharides, which are involved in cell structure, bacterial recognition and adhesion. Four enzymes involved in fermentation were all up-regulated in biofilms, as were those involved in the utilization of iron and sulfur sources. Among the 15 down-regulated genes, 11 encoded multiple terminal respiratory enzymes (the nitrate/nitrite reductase, TMAO reductase, DMSO reductase and hydrogenase). Therefore, the utilization of oligosaccharides, iron and sulfur, fermentation and

Table 1 Identification of Fnr binding sites^a in the promoter regions of differentially expressed genes (BF compared with PK)

Functional class	Target genes ^b	Transcription change ^c
Transcription, Translation	<i>rplKA, rplJL, rpsJ- rplCDWB- rpsS- rplV-rpsC-rplP- rpmC-rpsQ, rplNXE-rpsNH-rplFR-rpsE-rpmD-rplO-secY-rpmJ, rpsMKD-rpoA-rplQ, rplU-rpmA, raiA, rraA</i> <i>argS, folE-truA, ttcA, rpoE</i>	Down Up
Energy metabolism	<i>cydAB, ppc, pta-ackA, atpEFHAGDC, fbaA, glpX, gpmA, torY, torA, dmsABCD, nrfABCD, ppa, pfkA, napFDA, nqrABCDEF, hypBDE, hypF, eno, nudE-cysQ</i> <i>glpE-ybbN, can, cysJL</i>	Down Up
Carbohydrate metabolism	<i>pgk, pyk, tkt, frdABCD, tpiA, pckA, ilvB, mdh, gloA, hxpB, tal, fumC, focA-pflB, lpd-aceF</i> <i>fbp, APPSER1_RS05435, indK, lldD, gntR, APPSER1_RS09580-nanEKA-nagB</i>	Down Up
Amino acids	<i>metE, asnA, pepA, adhE, ilvE, cysK, proB, dapA, gdhA, argG, aspC, mmsB</i> <i>gshAB, tyrA, hisC, hisIE, hisG, metJ</i>	Down Up
Membrane transport	<i>APPSER1_RS06785, scrA, afuA, fruBKA, ptsH, ptsI-crr</i> <i>sbp-cysUWA, fhuCD, znuC, malk-lamb-malm, sitCD</i>	Down Up
Signal transduction	<i>hybOAB, soda, cydAB, ducB, eno, pfkA, frdA, hfq</i> <i>fnr, fbp, APPSER1_RS05435, htpG</i>	Down Up
Cofactors and Vitamins	<i>fabB, pdxST, pntAB</i> <i>folB, ribF, ribDEBA, hemaA, folE-truA, folC, lipA, cysGHDN</i>	Down Up
Lipid metabolism	<i>fabB, adhE</i> <i>adhP, glpQ, psd</i>	Down Up
Folding, sorting and degradation	<i>hfq, eno, pfkA</i> <i>moaCDE, rppH, pcnB-folk, tusE, htpG, tusBCD</i>	Down Up
Cellular community	<i>hfq, cyaA</i> <i>fis, pgaABCD, ribDEBA, APPSER1_RS00145</i>	Down Up
Replication and repair	<i>dnaE</i> <i>rnhA, nfo, ung</i>	Down Up
Nucleotide metabolism	<i>ushA, cpdB, pyrE, cyaA</i> <i>dtd, rsml</i>	Down Up
Virulence factor	<i>apxICA, apxIICA</i>	Down

Genes in bold indicate those also with Fis binding sites in the promoter regions.

^aThe Fnr motif used for searching was TTGATNWNMCKAH.

^bTarget genes were predicted from the MEME-FIMO online tool, p -value < 0.001.

^cTranscriptional changes of target genes were derived from differentially expressed genes in RNA-Seq data, Down, down-regulated, $\log_2FC \leq -1$, FDR < 0.05; Up, up-regulated, $\log_2FC \geq 1$, FDR < 0.05.

repressed anaerobic respiration may be involved in mediating the adhesion or aggregation of bacteria during *A. pleuropneumoniae* biofilm formation.

Biofilm-grown *A. pleuropneumoniae* showed reduced virulence in mice

To compare the virulence of biofilm and planktonic bacteria, mice were infected intranasally with log-phase biofilm and planktonic bacteria. A lethal dose of *A. pleuropneumoniae* (4×10^6 CFU) resulted in acute mortality in mice, with the earliest death occurring even within 12 h and the lethality stabilized within 72 h (Figure 6A). Compared with that infected by planktonic bacteria, the lethality of mice infected by biofilm-grown bacteria was significantly lower ($p < 0.05$), and the onset of mouse death was delayed in the biofilm infection group (Figure 6A). A sub-lethal dose (2×10^6 CFU) was also used

to assess bacterial colonization capacity. *A. pleuropneumoniae* proliferated rapidly in mice, with the numbers peaking near 12 h (Figure 6B). There was no significant difference in the bacterial load in vivo between BF and PK at 12 h or 48 h post-infection (Figure 6B). Bacteria were gradually cleared as the infection progressed, and it was seen that the BF-infected group had a higher number of bacteria surviving in vivo than PK at 72 h (Figure 6B). In summary, when used as an inoculum, *A. pleuropneumoniae* biofilm grown bacteria had reduced virulence in mice, and presented a more sustained in vivo colonization than PK.

Discussion

Bacteria living as biofilms is a common trait of prokaryotes. The structure of biofilm aggregates facilitates bacterial resistance to environmental stresses and survival.

Table 2 Identification of Fis binding sites^a in the promoter regions of differentially expressed genes (BF compared with PK)

Functional class	Target genes ^b	Transcription change ^c
Transcription, Translation	<i>rplNXE-rpsNH-rplIFR-rpsE-rpmD-rplO-secY-rpmJ</i> , <i>rpmBG</i> , <i>rplU-rpmA</i> , <i>rplKA</i> , <i>rpsP-rimM-trmD-rplS</i> , <i>rpsT</i> , <i>rpsB-tsf</i> , <i>rpsO</i> , <i>rplM-rpsI</i> , <i>rpsJ-rplCDWB-rpsS-rplV-rpsC-rplP-rpmC-rpsQ</i> , <i>rpsF-priB-rpsR-rplI</i> , <i>rpsL</i> , <i>rplJL</i> , <i>rpoZ</i> , <i>frz</i> , <i>raiA</i> , <i>rraA</i> <i>argS</i> , <i>rpoE</i> , <i>rimP-nusA-infB</i>	Down Up
Energy metabolism	<i>cydAB</i> , <i>ppc</i> , <i>pta-ackA</i> , <i>dmsABCD</i> , <i>napFDA</i> , <i>nrfABCD</i> , <i>ppa</i> , <i>pfkA</i> , <i>torY</i> , <i>glpX</i> , <i>eno</i> , <i>hypBDE</i> , <i>hypF</i> , <i>nqrABCDEF</i> , <i>nudE-cysQ</i> <i>glpE-ybbN</i> , <i>can</i> , <i>cysJL</i> , <i>fdhE</i>	Down Up
Carbohydrate metabolism	<i>pgk</i> , <i>tkt</i> , <i>frdABCD</i> , <i>tpiA</i> , <i>pckA</i> , <i>ilvB</i> , <i>mdh</i> , <i>hxpB</i> , <i>tal</i> , <i>manXYZ</i> , <i>fucO</i> , <i>lpd-aceF</i> <i>fbp</i> , <i>APPSER1_RS05435</i> , <i>indK</i> , <i>lldD</i> , <i>APPSER1_RS09580-nanEKA-nagB</i> , <i>gntR</i>	Down Up
Amino acids	<i>glmS</i> , <i>adhE</i> , <i>ilvE</i> , <i>cysK</i> , <i>proB</i> , <i>dapA</i> , <i>gdhA</i> , <i>argG</i> , <i>aspC</i> , <i>mmsB</i> <i>gshAB</i> , <i>tyrA</i> , <i>hisC</i> , <i>hisIE</i> , <i>hisD</i> , <i>APPSER1_RS10930</i>	Down Up
Membrane transport	<i>scrA</i> , <i>afuA</i> , <i>fruBKA</i> , <i>ptsH</i> , <i>ptsI-crr</i> , <i>xylGH</i> , <i>cbiKLM</i> , <i>ompW</i> <i>sbp-cysUWA</i> , <i>fhuCD</i> , <i>znuC</i> , <i>flrY</i> , <i>sitCD</i>	Down Up
Signal transduction	<i>hybOAB</i> , <i>sodA</i> , <i>cydAB</i> , <i>ducB</i> , <i>eno</i> , <i>pfkA</i> , <i>frdA</i> , <i>hfq</i> <i>fnr</i> , <i>fbp</i> , <i>htpG</i>	Down Up
Cofactors and Vitamins	<i>ushA</i> , <i>pdxST</i> , <i>pntAB</i> , <i>ilvB</i> , <i>ilvE</i> <i>folB</i> , <i>ribF</i> , <i>ribDEBA</i> , <i>hemA</i> , <i>folE-truA</i> , <i>folC</i> , <i>lipA</i> , <i>cysGHDN</i>	Down Up
Lipid metabolism	<i>adhE</i> <i>adhP</i> , <i>glpQ</i> , <i>psd</i>	Down Up
Folding, sorting and degradation	<i>hfq</i> , <i>eno</i> , <i>pfkA</i> , <i>secG</i> <i>rppH</i> , <i>pcnB-folK</i> , <i>tusE</i> , <i>htpG</i> , <i>tusBCD</i>	Down Up
Cellular community	<i>hfq</i> , <i>secG</i> <i>fis</i> , <i>ribDEBA</i> , <i>dksA</i> , <i>APPSER1_RS00145</i>	Down Up
Replication and repair	<i>dnaE</i> <i>hold-rimI-srmB-pdxH</i> , <i>dnaG</i> , <i>rnhA</i> , <i>nfo</i>	Down Up
Nucleotide metabolism	<i>ushA</i> , <i>cpdB</i> <i>trmA</i> , <i>rsml</i>	Down Up
Virulence factor	<i>apxIIICA</i>	Down

Genes in bold indicate those also with Fnr binding sites in the promoter regions.

^a The Fis motif used for searching was GNNBRWWWWTVNNCRN.

^b Target genes were predicted from the MEME-FIMO online tool, *p*-value < 0.001.

^c Transcriptional changes of target genes were derived from differentially expressed genes in RNA-Seq data, Down, down-regulated, $\log_2FC \leq -1$, FDR < 0.05; Up, up-regulated, $\log_2FC \geq 1$, FDR < 0.05.

Persistent and/or latent infections arising from the biofilm mode of growth have become a major factor in the persistence of disease and its re-emergence [46]. As an important respiratory pathogen, it has been reported that most field isolates of *A. pleuropneumoniae* form biofilms in the laboratory when initially isolated [17]. In pigs, aggregates of *A. pleuropneumoniae* in host lungs is considered a biofilm mode of growth, which may act as a reservoir for outbreaks of infection when exposed to stressors or when other pathogens evade the host [18]. Therefore, the biofilm mode of growth can be considered as facilitating survival of *A. pleuropneumoniae* in the host. In this study, we compared the growth features and gene expression patterns of *A. pleuropneumoniae* grown in biofilms with planktonic cells.

A simple in vitro culture method in 12-well plates was used to generate stable *A. pleuropneumoniae* biofilms, and there were obvious differences in growth curves and morphology, compared with that of the planktonic bacteria obtained from shake cultures (Figure 1). Through construction and comparative analysis of WT, Δpga and complimentary strains, it was confirmed that PNAG, a known polysaccharide component of EPS for biofilm formation of many bacteria, was critical for *A. pleuropneumoniae* biofilm formation (Figure 2). Similarly, it was also confirmed that dispersin B (encoded by *dspB*), an enzyme that degrades PNAG was also involved in the regulation of *A. pleuropneumoniae* biofilm formation (Figure 2). These results are consistent with previous studies [24, 25].

Table 3 Identification of H-NS binding sites^a in the promoter regions of differentially expressed genes (BF compared with PK)

Functional class	Target genes ^b	Transcription change ^c
Transcription, Translation	<i>rpsP-rimM-trmD-rplS, psG-fusA-tuf, rpsT, rpsL</i>	Down
	<i>rimP-nusA-infB</i>	Up
Energy metabolism	<i>ppc, pta-ackA, nrfABCD, atpEFHAGDC, glpX, fumC</i>	Down
	<i>fdhE, fdhC, can</i>	Up
Carbohydrate metabolism	<i>tpiA, mdh, tal</i>	Down
	<i>lld</i>	Up
Amino acids	<i>mmsB, cysK, metE, ackA</i>	Down
	<i>marC, filY</i>	Up
Membrane transport	<i>afuA</i>	Down
	<i>fhuCD, fliY, sitCD</i>	Up
Signal transduction	<i>hfq, htpG</i>	Up
Cofactors and Vitamins	<i>fabB, pntAB</i>	Down
	<i>folB, ribF, ribDEBA, hema, folC, lipA</i>	Up
Lipid metabolism	<i>fabB</i>	Down
	<i>glpQ</i>	Up
Folding, sorting and degradation	<i>hfq, secG</i>	Down
	<i>rppH, htpG</i>	Up
Cellular community	<i>cyaA, secG, hfq</i>	Down
	<i>fis, cpdA, APPSER1_RS00145</i>	Up
Replication and repair	<i>rnhA, nfo</i>	Up
Nucleotide metabolism	<i>ushA, cpdB, pyrE, purl-APPSER1_RS09210, cyaA</i>	Down
	<i>cpdA, rsml</i>	Up

^a The H-NS motif used for searching was RATAWH.

^b Target genes were predicted from the MEME-FIMO online tool, *p*-value < 0.001.

^c Transcriptional changes of target genes were derived from differentially expressed genes in RNA-Seq data, Down, down-regulated, $\log_2FC \leq -1$, FDR < 0.05; Up, up-regulated, $\log_2FC \geq 1$, FDR < 0.05.

Numerous genes have been reported to affect *A. pleuropneumoniae* biofilm formation [27–32]. Among these genes, the H-NS and the TCS CpxAR have been validated to direct regulate the genes *pgaABCD* encoding PNAG synthesis proteins [26, 32]. For other genes, it is still relatively unknown how they influence *A. pleuropneumoniae* formation and/or maintenance. In this study, we used RNA-seq analysis to compare the gene expression of *A. pleuropneumoniae* biofilm and planktonic cultures. This contrasts with a previous study also with 4074, that used microarray hybridization to compare transcriptional profiles of *A. pleuropneumoniae* biofilms at different stages in a drip-flow apparatus and also under static culture [33]. The results indicated that some genes involved in energy metabolism were down-regulated and genes encoding transporters were up-regulated in *A. pleuropneumoniae* biofilms, some of which were also found in this work. For example, the down-regulated genes *ppc* (encodes phosphoenolpyruvate carboxylase), *pckA* (encodes phosphoenolpyruvate carboxykinase), *dmsABC* (encodes anaerobic dimethyl sulfoxide reductase) and

genes encoding ribosomal proteins, and the up-regulated genes *znuC* (zinc ABC transporter ATP-binding protein, *fdhC* (formate/nitrite transporter family protein) and *ribD* (5-amino-6-(5-phosphoribosylamino) uracil reductase) were also identified in this study. Unlike hybridization-based microarray technology, RNA-Seq has no upper limit of quantification, which correlates with the number of sequences obtained, and thus it can detect a large range of dynamic expression levels of transcripts [47]. In addition, the advantages of high resolution and low background signal of RNA-seq allow for a high level of reproducibility of gene expression detections, as verified by qRT-PCR in this work (Figures 3C, D). Four times of the number of differentially expressed genes in biofilms were identified in this study compared to that using microarray hybridization, thus expanding our understanding of gene transcription profile of biofilm-grown *A. pleuropneumoniae* (Figure 5).

The gene expression of *A. pleuropneumoniae* grown in biofilms was distinct from growth planktonically. In general, many different metabolic pathways and their

Table 4 The differentially expressed genes of BF compared with Δpga

Function	Gene_ID	Gene_Name	Description
Up-regulated genes/operons ($\log_2FC \geq 1$, FDR < 0.05)			
Carbohydrate metabolism	APPSER1_RS05460-APPSER1_RS05465	<i>galTK</i>	galactokinase
	APPSER1_RS07965-APPSER1_RS07970	<i>mglAC</i>	galactose/methyl galactoside ABC transporter
	APPSER1_RS09115-APPSER1_RS09120	<i>manYZ</i>	mannose PTS system
	APPSER1_RS09135	<i>idhK</i>	gluconokinase
	APPSER1_RS06715-APPSER1_RS06725	<i>malM-APPSER1_RS06720-malK</i>	maltose/maltodextrin ABC transporter
	APPSER1_RS06730, APPSER1_RS06740	<i>malE-malG</i>	maltose/maltodextrin ABC transporter
	APPSER1_RS05415	APPSER1_RS05415	glycosyltransferase
	APPSER1_RS09220	<i>fucRIKU</i>	L-fucose isomerase; L-fuculokinase; L-fucose mutarotase
	APPSER1_RS09580-APPSER1_RS09605	APPSER1_RS09580- <i>nanEKA-nagBA</i>	N-acetylmannosamine kinase; N-acetylneuraminase lyase; glucosamine-6-phosphate deaminase; N-acetylglucosamine-6-phosphate deacetylase
Fermentation	APPSER1_RS02385-APPSER1_RS02390	<i>lldEF</i>	L-lactate dehydrogenase
	APPSER1_RS02395	<i>lctP</i>	L-lactate permease
	APPSER1_RS10140	<i>lldD</i>	FMN-dependent L-lactate dehydrogenase LldD
Transporter	APPSER1_RS10665	<i>adhP</i>	alcohol dehydrogenase AdhP
	APPSER1_RS07470-APPSER1_RS07490	<i>ccmEDCBA</i>	cytochrome c maturation protein; heme exporter protein
	APPSER1_RS04515-APPSER1_RS04525	APPSER1_RS04515-APPSER1_RS04525	dipeptide/oligopeptide/nickel ABC transporter
	APPSER1_RS09260-APPSER1_RS09265	APPSER1_RS09260-APPSER1_RS09265	amino acid ABC transporter
	APPSER1_RS09375	<i>ulaAB</i>	PTS ascorbate transporter
	APPSER1_RS07040-APPSER1_RS07045	<i>mIaEF</i>	phospholipid ABC transporter
	APPSER1_RS10020	<i>glpT</i>	glycerol-3-phosphate transporter
	APPSER1_RS10940-APPSER1_RS10945	<i>fhuCD</i>	iron-siderophore ABC transporter
	APPSER1_RS10115-APPSER1_RS10130	<i>sbp-cysTW-cysA</i>	sulfate ABC transporter
	APPSER1_RS10085-APPSER1_RS10090	<i>cysJl</i>	assimilatory sulfite reductase; assimilatory sulfite reductase
Reductase	APPSER1_RS10095-APPSER1_RS10110	<i>cysGHDN</i>	phosphoadenylyl-sulfate reductase
	APPSER1_RS10595	<i>cpdA</i>	3',5'-cyclic-AMP phosphodiesterase
Others	APPSER1_RS02045-APPSER1_RS02050	<i>ribDE</i>	uracil reductase RibD; riboflavin synthase
	APPSER1_RS05435	<i>katE</i>	catalase
	APPSER1_RS10970	<i>hisG, hisD, hisC</i>	ATP phosphoribosyltransferase; histidinol dehydrogenase; histidinol-phosphate transaminase
Down-regulated genes/operons ($\log_2FC \leq -1$, FDR < 0.05)			
Reductase	APPSER1_RS00525-APPSER1_RS00530	<i>nrfAB</i>	nitrite reductase
	APPSER1_RS07905-APPSER1_RS07915	<i>napFDA</i>	nitrate reductase
	APPSER1_RS09175-APPSER1_RS09190	<i>dmsABCD</i>	anaerobic dimethyl sulfoxide reductase
	APPSER1_RS03675	<i>torY</i>	trimethylamine-N-oxide reductase
	APPSER1_RS07240	<i>hyaA</i>	hydrogenase 2

components were down-regulated in biofilms. These included, enzymes involved in glycolysis, pentose phosphate pathway, TCA cycle and the oxidative phosphorylation pathway. In addition to aerobic respiration,

genes involved in anaerobic respiration using alternative electrons (nitrate, DMSO TMSO) were also down-regulated. In contrast, sulfur and histidine metabolism, iron transport and coenzyme synthesis were up-regulated.

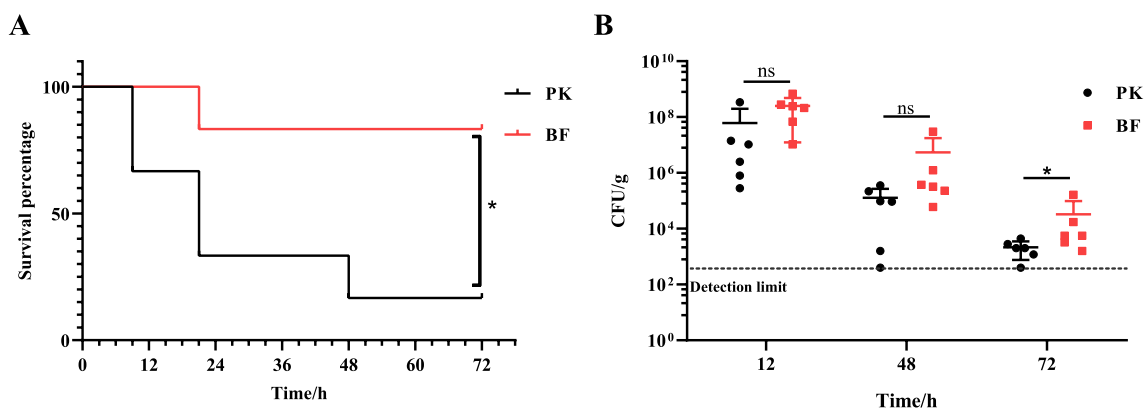


Figure 6 Pathogenicity of *A. pleuropneumoniae* biofilm (BF) and planktonic (PK) grown bacteria for mice. **A** Survival rates of mice (6 per group) intranasally infected with PK and BF, respectively, at 4×10^6 CFU in 20 μ L for each mouse. Log rank (Mantel-Cox) test was performed for statistical analysis (*, $p < 0.05$). **B** Bacterial loads in the lungs of mice intranasally infected with PK or BF at a dose of 2×10^6 CFU per mouse. Dotted line: the limit of detection (400 CFU/g). Two-tailed Mann–Whitney test was used for statistical analysis (*, $p < 0.05$; ns: not significant).

Biofilm grown bacteria had significantly up-regulated PNAG synthesis and amino sugar metabolic pathways, which are essential for the formation of cell wall and EPS components of biofilm [48]. These results suggest that *A. pleuropneumoniae* growing in biofilms have a reduced metabolism compared to their planktonic counterparts, reprogramming of metabolic reactions, and a shift to synthesis and translocation of the cell wall and EPS components, most likely occurring to enable survival to stress.

Antibiotic resistance often contributes to the difficulty of biofilm eradication [21]. It has been reported that *A. pleuropneumoniae* field isolates contained multiple antibiotic resistance genes and were positively correlated with their ability to form biofilms [49]. In our study, many antibiotic resistance genes were up-regulated in biofilms (Additional file 4), including *tet* (APPSER1_RS02405) encoding a tetracycline resistance efflux pump [50], *vcaM* (APPSER1_RS06625) encoding an ABC-type multidrug efflux pump [51], *macB* (APPSER1_RS03395) encoding a macrolide transport system ATP-binding/permease protein [52], *rarD* (APPSER1_RS05710) encoding a predicted chloramphenicol resistance permease, and *marC* (APPSER1_RS06555) encoding a predicted multiple antibiotic resistance protein. In addition, a low growth rate also potentially contributes to resistance to antibiotics. Traditional antibiotics usually target bacterial components essential for proliferation, such as proteins involved in cell wall synthesis, DNA synthesis and protein translation. Metabolic processes have also been found to be affected by antibiotics and directly linked to antibiotic efficacy. Bactericidal antibiotics can kill bacteria by inducing their respiration [53]. Biocides and antibiotics can cause elevated ATP and respiration in bacteria by the PTS and the cAMP-Crp cascade, resulting

in over-production of reactive oxygen species to a lethal concentration [54]. Therefore, the decreased metabolic activity and ATP biosynthesis found in the biofilm the “resting-mode” can make bacteria more tolerance to antibiotics [4].

It was noted that the genes encoding the major virulence genes of *A. pleuropneumoniae*, the *apxIA* and *apxIIA*, were significantly down-regulated in biofilms. *A. pleuropneumoniae* has four types of RTX toxins, the ApxI, ApxII, ApxIII and ApxIV [15]. The strain used in this study is a virulent strain of serovar 1, which possess both ApxI and ApxII that are both necessary for full virulence of *A. pleuropneumoniae* [55]. Consistent with the down-regulation of the structural genes of both ApxI and ApxII, when used as inocula, biofilm grown bacteria showed reduced lethality for mice (Figure 6A). When the mice were infected with sub-lethal doses, the bacterial numbers recovered from the lungs showed no significant difference between biofilm and planktonic bacteria groups up to 48 h post-infection (Figure 6B), indicating that the difference in lethality was not related to differences in bacterial proliferation in vivo. At 72 h post-infection, the viable number in the lungs of mice infected with biofilm was higher than that infected with planktonic bacteria (Figure 6B), suggesting that the survival time of biofilm was longer in vivo. These results indicate that *A. pleuropneumoniae* growing as as biofilm are less virulent, which is in agreement with previous studies that *A. pleuropneumoniae* biofilm grown cells trigger weaker immune responses [23], and negatively correlates with the severity of lung lesions of pigs [17]. Therefore, it can be inferred that *A. pleuropneumoniae* growing in biofilms down-regulate some main virulence factors and basic metabolic activities, while up-regulating the expression

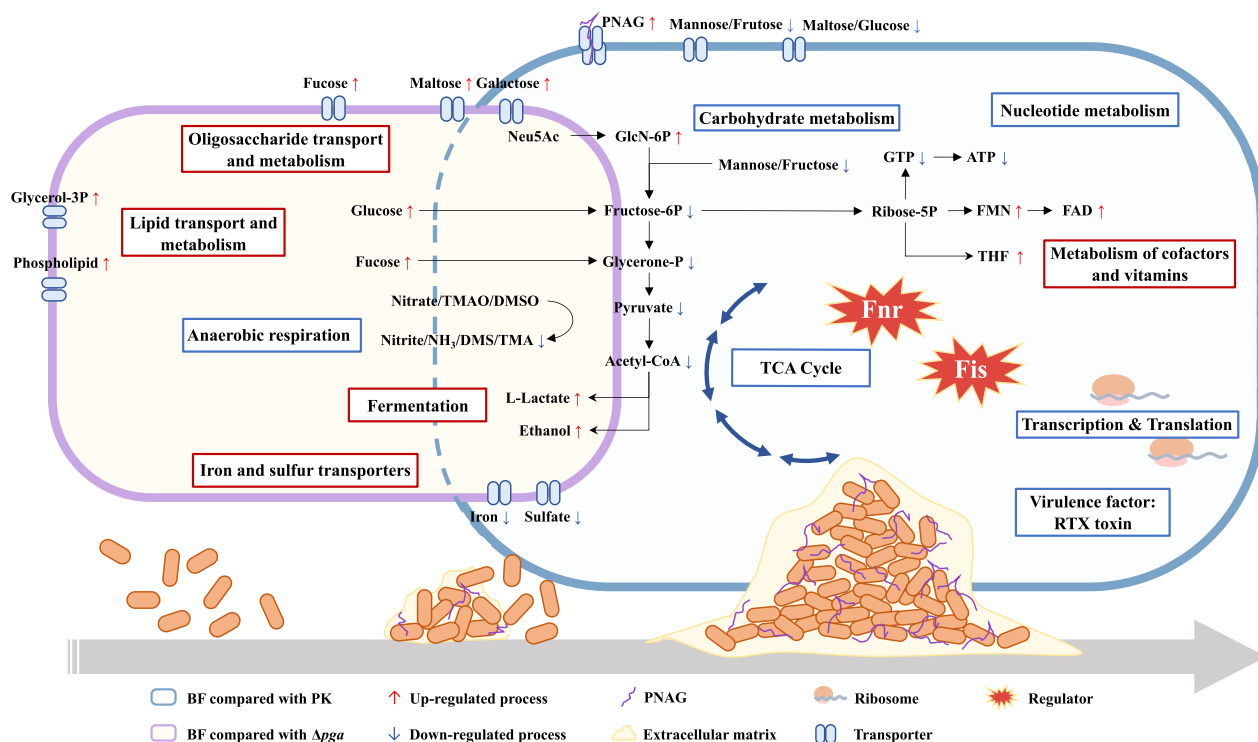


Figure 7 Metabolic changes of *A. pleuropneumoniae* living in biofilms compared with planktonic bacteria. The contents in the purple outlined cell indicate the pathways closely related to adhesion and aggregation during biofilm formation. The pathways in blue outlined cell indicate those altered during the biofilm mode of growth. Red box: up-regulated pathways. Blue box: down-regulated pathways.

of antibiotic resistance genes and those involved in the maintenance of EPS structures, which can facilitate long-lasting survival in the host.

The biofilm mode of growth is known to be dependent on signal transduction proteins and regulators [8–10]. In this study, in addition to H-NS that was up-regulated in biofilms, two other regulators were identified to be up-regulated, Fnr (HlyX) and Fis. Up-regulated expression of Fnr may be activated by the anaerobic environment inside the biofilm [56]. Many differentially expressed genes involved in the metabolic pathways in *A. pleuropneumoniae* biofilms have been reported to be regulated by Fnr [57]. Proteomic and transcriptomic analyses showed that Fnr (HlyX) induces the expression of genes encoding alternative terminal reductases and hydrogenases which are functional in the anaerobic metabolism of *A. pleuropneumoniae* [57]. However, in this study, Fnr was induced in biofilms, but a lot of its target genes involved in energy and carbohydrate metabolism, including multiple terminal respiratory enzymes, mannose/fructose transporter and the enzymes involved in TCA cycle were down-regulated (Table 1). Simultaneously, *fis* encoding the global regulator Fis [45], was also up-regulated. By analyzing the binding motifs of Fis and Fnr in the database in the upstream regions of the differentially

expressed genes in biofilms, we found that most of the upstream regions of these genes had binding sites of both Fis and Fnr, with more genes potentially regulated by Fis (Tables 1, 2). As a typical nucleoid associated protein that functions by binding to specific DNA sequences, Fis has the ability to mask the Fnr binding site, thereby inhibiting the activity of Fnr on the target genes [58, 59]. In *E. coli*, a combined RNA-seq and ChIP-seq analysis has illustrated the extensive role of Fis in regulation of sugar metabolism and transport, as well as the genes involved in cell division, bacteriocin transport and biofilm formation [60]. The overlapping of the regulons of *A. pleuropneumoniae* Fis and Fnr provides an explanation for differential regulation of Fnr target genes in the biofilm transcriptome. Binding of Fis with *nrf* and *nir* promoters is known to inhibit Fnr regulation [61, 62]. Additionally, *A. pleuropneumoniae* Fis and Fnr may regulate each other's expression since there are binding sites of each other in the upstream regions of their coding genes (Tables 1, 2). A detailed analysis of the cross-regulation of Fis and Fnr on *A. pleuropneumoniae* biofilm gene expression will be the subject of further study.

At present, effective strategies to prevent biofilm formation include the inhibition of sessile bacterial adhesion and initial structure formation by interfering with

EPS secretion, such as the utilization of peptidoglycan hydrolase [63], and the use of an antibody against specific EPS components [64]. Lysis of intercellular junctions using DNases and proteases [65, 66] and release of antibiotic-sensitive individual cells from biofilm aggregates by changing the levels of signaling molecules [67, 68] have also been reported to be effective for biofilm treatment. Based on the metabolic behavior of *A. pleuropneumoniae* growing in biofilms, according to the gene expression profile, we speculate that reducing the availability of specific nutrients including oligosaccharides (sialic acid, fucose, galactose.), amino acids, iron or sulfur sources may reduce the adhesion and aggregation of *A. pleuropneumoniae* and the formation of biofilms.

In summary, the growth features, morphology, gene expression and virulence of *A. pleuropneumoniae* biofilm grown bacteria were compared with their planktonic counterparts. The results confirmed that *A. pleuropneumoniae* self-aggregated and adhered to surfaces and secreted EPS to form biofilm. The gene expression profiles of *A. pleuropneumoniae* in biofilms were altered extensively, suggesting a lower level of basic metabolic activity, and a fermentation mode of growth accompanied by expression of genes for major EPS synthesis (Figure 7). The regulators Fnr and Fis appear to coordinately have a global regulatory role in maintaining the metabolism of *A. pleuropneumoniae* biofilms. Down-regulation of known virulence genes, e.g., the Apx toxins, is consistent with the reduced virulence of biofilm grown bacteria compared to their planktonic counterparts. These results increase our understanding of *A. pleuropneumoniae* biofilm regulation and development of its clearance strategies.

Supplementary Information

The online version contains supplementary material available at <https://doi.org/10.1186/s13567-023-01173-x>.

Additional file 1: Validation of the mutants Δpga , $\Delta dspB$ and their complementary strains. (A-B) gDNA was extracted from *A. pleuropneumoniae* wild type (WT), Δpga , $\Delta dspB$ and their complementary strains. (C-D) RNA was extracted from *A. pleuropneumoniae* WT, Δpga , $\Delta dspB$ and their complementary strains, and cDNA was synthesized by RT-PCR after gDNA erasure. PCR identification was performed using the indicated primers with gDNA or cDNA as template. Primers *pga*-UF and *pga*-DR bind to the upstream and downstream regions of the *pga* operon, respectively; the primers Δpga -F/R amplify the internal fragment of the *pga* operon; Primers APPSER1_RS10490 -F/R and APPSER1_RS10515-F/R are used to amplify the upstream and downstream genes of *pga* operon, respectively. Primers *dspB*-F/R amplify the full-length fragment of the *dspB*; Primers $\Delta dspB$ -F/R amplify the internal fragment of the *dspB*; Primers APPSER1_RS05990-F/R and APPSER1_RS06000-F/R are used to amplify the upstream and downstream genes of *dspB*, respectively.

Additional file 2: Growth curves of *A. pleuropneumoniae* wild type (WT), Δpga , $\Delta dspB$ and their complementary strains. The absorbances

at OD_{600nm} of bacterial cultures were determined every 2 h. Data are shown as means \pm SD from three independent replicates.

Additional file 3: Bacterial strains, plasmids and primers used in this study.

Additional file 4: The differentially expressed genes of BF compared with PK and analysis of transcription factor binding sites on their promoters.

Additional file 5: The differentially expressed genes of BF compared with Δpga .

Acknowledgements

We thank Majorbio Technology Co., Ltd for providing technical support for RNA-seq and analysis.

Authors' contributions

Conception of the work: LL; laboratory techniques: QZ, LP, WH and HC; acquisition, analysis and interpretation of data: QZ, HT, and QH; preparation of the manuscript: QZ, LL and PL. funding acquisition and project administration: LL, RZ, XC and PL. All authors read and approved the final manuscript.

Funding

This work was supported by the National Key Research and Development Program of China (2021YFD1800404), National Natural Science Foundation of China (31572535), Hubei Provincial Central Guidance Local Science and Technology Development Project of China (No.2020ZYD029), and the UK Biotechnology and Biological Sciences Research Council (BB/S019901/1).

Availability of data and materials

The dataset supporting the conclusions of this article is available in the NCBI's Gene Expression Omnibus repository and are accessible through GEO Series accession number GSE221940.

Declarations

Ethics approval and consent to participate

Kunming mice were purchased from Laboratory Animal Centre, Huazhong Agriculture University, Wuhan, China. All animal procedures abide by the ethical principles of animal welfare and were performed according to protocols approved by the Ethic Committee of Huazhong Agricultural University (HZAUMO-2023-0001).

Competing interests

The authors declare that they have no competing interests.

Received: 28 February 2023 Accepted: 23 April 2023

Published online: 26 May 2023

References

- Chua SL, Liu Y, Yam JK, Chen Y, Vejborg RM, Tan BG, Kjelleberg S, Tolker-Nielsen T, Givskov M, Yang L (2014) Dispersed cells represent a distinct stage in the transition from bacterial biofilm to planktonic lifestyles. *Nat Commun* 5:4462
- Trubenová B, Roizman D, Moter A, Rolff J, Regoes RR (2022) Population genetics, biofilm recalcitrance, and antibiotic resistance evolution. *Trends Microbiol* 30:841–852
- Vuong C, Voyich JM, Fischer ER, Braughton KR, Whitney AR, DeLeo FR, Otto M (2004) Polysaccharide intercellular adhesin (PIA) protects *Staphylococcus epidermidis* against major components of the human innate immune system. *Cell Microbiol* 6:269–275
- Hall CW, Mah TF (2017) Molecular mechanisms of biofilm-based antibiotic resistance and tolerance in pathogenic bacteria. *FEMS Microbiol Rev* 41:276–301

5. Smolarz M, Zawrotniak M, Satala D, Rapala-Kozik M (2021) Extracellular nucleic acids present in the *Candida albicans* biofilm trigger the release of neutrophil extracellular traps. *Front Cell Infect Microbiol* 11:681030
6. Paharik AE, Horswill AR (2016) The staphylococcal biofilm: adhesins, regulation, and host response. *Microbiol Spectr* 4:4.2.06
7. Zhang T, Zhu J, Xu J, Shao H, Zhou R (2020) Regulation of (p)ppGpp and its homologs on environmental adaptation, survival, and pathogenicity of *Streptococci*. *Front Microbiol* 11:1842
8. Labrie J, Pelletier-Jacques G, Deslandes V, Ramjeet M, Auger E, Nash JH, Jacques M (2010) Effects of growth conditions on biofilm formation by *Actinobacillus pleuropneumoniae*. *Vet Res* 41:3
9. Shrout JD, Chopp DL, Just CL, Hentzer M, Givskov M, Parsek MR (2006) The impact of quorum sensing and swarming motility on *Pseudomonas aeruginosa* biofilm formation is nutritionally conditional. *Mol Microbiol* 62:1264–1277
10. Fazli M, Almblad H, Rytbke ML, Givskov M, Eberl L, Tolker-Nielsen T (2014) Regulation of biofilm formation in *Pseudomonas* and *Burkholderia* species. *Environ Microbiol* 16:1961–1981
11. Schilcher K, Horswill AR (2020) Staphylococcal biofilm development: structure, regulation, and treatment strategies. *Microbiol Mol Biol Rev* 84:e00026-e119
12. Hengge R (2009) Principles of c-di-GMP signalling in bacteria. *Nat Rev Microbiol* 7:263–273
13. Vandana DS (2022) Genetic regulation, biosynthesis and applications of extracellular polysaccharides of the biofilm matrix of bacteria. *Carbohydr Polym* 291:119536
14. Bossé JT, Janson H, Sheehan BJ, Beddek AJ, Rycroft AN, Kroll JS, Langford PR (2002) *Actinobacillus pleuropneumoniae*: pathobiology and pathogenesis of infection. *Microbes Infect* 4:225–235
15. Sassu EL, Bossé JT, Tobias TJ, Gottschalk M, Langford PR, Hennig-Pauka I (2018) Update on *Actinobacillus pleuropneumoniae*-knowledge, gaps and challenges. *Transbound Emerg Dis* 65:72–90
16. Gottschalk M (2015) The challenge of detecting herds sub-clinically infected with *Actinobacillus pleuropneumoniae*. *Vet J* 206:30–38
17. Aper D, Frömbling J, Bağcıoğlu M, Ehling-Schulz M, Hennig-Pauka I (2020) Comparison of metabolic adaptation and biofilm formation of *Actinobacillus pleuropneumoniae* field isolates from the upper and lower respiratory tract of swine with respiratory disease. *Vet Microbiol* 240:108532
18. Tremblay YDN, Labrie J, Chenier S, Jacques M (2017) *Actinobacillus pleuropneumoniae* grows as aggregates in the lung of pigs: is it time to refine our *in vitro* biofilm assays? *Microb Biotechnol* 10:756–760
19. Loera-Muro A, Ramírez-Castillo FY, Moreno-Flores AC, Martin EM, Avelar-González FJ, Guerrero-Barrera AL (2021) *Actinobacillus pleuropneumoniae* surviving on environmental multi-species biofilms in swine farms. *Front Vet Sci* 8:722683
20. Loera-Muro A, Jacques M, Avelar-González FJ, Labrie J, Tremblay YD, Oropeza-Navarro R, Guerrero-Barrera AL (2016) Auxotrophic *Actinobacillus pleuropneumoniae* grows in multispecies biofilms without the need for nicotinamide-adenine dinucleotide (NAD) supplementation. *BMC Microbiol* 16:128
21. Hathroubi S, Loera-Muro A, Guerrero-Barrera AL, Tremblay YDN, Jacques M (2018) *Actinobacillus pleuropneumoniae* biofilms: role in pathogenicity and potential impact for vaccination development. *Anim Health Res Rev* 19:17–30
22. Wang Y, Gong S, Dong X, Li J, Grenier D, Yi L (2020) *In vitro* mixed biofilm of *Streptococcus suis* and *Actinobacillus pleuropneumoniae* impacts antibiotic susceptibility and modulates virulence factor gene expression. *Front Microbiol* 11:507
23. Hathroubi S, Beaudry F, Provost C, Martelet L, Segura M, Gagnon CA, Jacques M (2016) Impact of *Actinobacillus pleuropneumoniae* biofilm mode of growth on the lipid A structures and stimulation of immune cells. *Innate Immun* 22:353–362
24. Izano EA, Sadovskaya I, Vinogradov E, Mulks MH, Veliyagounder K, Ragu-nath C, Kher WB, Ramasubbu N, Jabbouri S, Perry MB, Kaplan JB (2007) Poly-N-acetylglucosamine mediates biofilm formation and antibiotic resistance in *Actinobacillus pleuropneumoniae*. *Microb Pathog* 43:1–9
25. Kaplan JB, Veliyagounder K, Ragu-nath C, Rohde H, Mack D, Knobloch JK, Ramasubbu N (2004) Genes involved in the synthesis and degradation of matrix polysaccharide in *Actinobacillus actinomycetemcomitans* and *Actinobacillus pleuropneumoniae* biofilms. *J Bacteriol* 186:8213–8220
26. Bossé JT, Sinha S, Li MS, O'Dwyer CA, Nash JH, Rycroft AN, Kroll JS, Langford PR (2010) Regulation of *pga* operon expression and biofilm formation in *Actinobacillus pleuropneumoniae* by sigmaE and H-NS. *J Bacteriol* 192:2414–2423
27. Li L, Xu Z, Zhou Y, Li T, Sun L, Chen H, Zhou R (2011) Analysis on *Actinobacillus pleuropneumoniae* LuxS regulated genes reveals pleiotropic roles of LuxS/AI-2 on biofilm formation, adhesion ability and iron metabolism. *Microb Pathog* 50:293–302
28. Li L, Zhou R, Li T, Kang M, Wan Y, Xu Z, Chen H (2008) Enhanced biofilm formation and reduced virulence of *Actinobacillus pleuropneumoniae* luxS mutant. *Microb Pathog* 45:192–200
29. Buettner FF, Maas A, Gerlach GF (2008) An *Actinobacillus pleuropneumoniae* *arcA* deletion mutant is attenuated and deficient in biofilm formation. *Vet Microbiol* 127:106–115
30. Li L, Zhu J, Yang K, Xu Z, Liu Z, Zhou R (2014) Changes in gene expression of *Actinobacillus pleuropneumoniae* in response to anaerobic stress reveal induction of central metabolism and biofilm formation. *J Microbiol* 52:473–481
31. Li G, Xie F, Zhang Y, Bossé JT, Langford PR, Wang C (2015) Role of (p) ppGpp in viability and biofilm formation of *Actinobacillus pleuropneumoniae* S8. *PLoS One* 10:e0141501
32. Li H, Liu F, Peng W, Yan K, Zhao H, Liu T, Cheng H, Chang P, Yuan F, Chen H, Bei W (2018) The CpxA/CpxR two-component system affects biofilm formation and virulence in *Actinobacillus pleuropneumoniae*. *Front Cell Infect Microbiol* 8:72
33. Tremblay YD, Deslandes V, Jacques M (2013) *Actinobacillus pleuropneumoniae* genes expression in biofilms cultured under static conditions and in a drip-flow apparatus. *BMC Genomics* 14:364
34. Zhang Q, Tang H, Yan C, Han W, Peng L, Xu J, Chen X, Langford PR, Bei W, Huang Q, Zhou R, Li L (2022) The metabolic adaptation in response to nitrate is critical for *Actinobacillus pleuropneumoniae* growth and pathogenicity under the regulation of NarX/P. *Infect Immun* 90:e0023922
35. Liu J, Hu L, Xu Z, Tan C, Yuan F, Fu S, Cheng H, Chen H, Bei W (2015) *Actinobacillus pleuropneumoniae* two-component system QseB/QseC regulates the transcription of PilM, an important determinant of bacterial adherence and virulence. *Vet Microbiol* 177:184–192
36. Bossé JT, Durham AL, Rycroft AN, Kroll JS, Langford PR (2009) New plasmid tools for genetic analysis of *Actinobacillus pleuropneumoniae* and other pasteurellaceae. *Appl Environ Microbiol* 75:6124–6131
37. Hermann T (2015) Non-coding RNA: antibiotic tricks a switch. *Nature* 526:650–651
38. Plumbbridge J, Vimr E (1999) Convergent pathways for utilization of the amino sugars N-acetylglucosamine, N-acetylmannosamine, and N-acetylneuraminic acid by *Escherichia coli*. *J Bacteriol* 181:47–54
39. Whitney JC, Howell PL (2013) Synthase-dependent exopolysaccharide secretion in Gram-negative bacteria. *Trends Microbiol* 21:63–72
40. Anderson MS, Raetz CR (1987) Biosynthesis of lipid precursors in *Escherichia coli*: a cytoplasmic acyltransferase that converts UDP-N-acetylglucosamine to UDP-3-O-(R-3-hydroxymyristoyl)-N-acetylglucosamine. *J Biol Chem* 262:5159–5169
41. Spiro S, Guest JR (1990) FNR and its role in oxygen-regulated gene expression in *Escherichia coli*. *FEMS Microbiol Rev* 6:399–428
42. MacInnes JI, Kim JE, Lian CJ, Soltes GA (1990) *Actinobacillus pleuropneumoniae* *hlyX* gene homology with the *fnr* gene of *Escherichia coli*. *J Bacteriol* 172:4587–4592
43. Frey J (1995) Virulence in *Actinobacillus pleuropneumoniae* and RTX toxins. *Trends Microbiol* 3:257–261
44. Ball CA, Osuna R, Ferguson KC, Johnson RC (1992) Dramatic changes in Fis levels upon nutrient upshift in *Escherichia coli*. *J Bacteriol* 174:8043–8056
45. Kahramanoglou C, Seshasayee AS, Prieto AI, Ibberson D, Schmidt S, Zimmermann J, Benes V, Fraser GM, Luscombe NM (2011) Direct and indirect effects of H-NS and Fis on global gene expression control in *Escherichia coli*. *Nucleic Acids Res* 39:2073–2091
46. Koo H, Allan RN, Howlin RP, Stoodley P, Hall-Stoodley L (2017) Targeting microbial biofilms: current and prospective therapeutic strategies. *Nat Rev Microbiol* 15:740–755
47. Wang Z, Gerstein M, Snyder M (2009) RNA-Seq: a revolutionary tool for transcriptomics. *Nat Rev Genet* 10:57–63
48. Winkler JD, Garcia C, Olson M, Callaway E, Kao KC (2014) Evolved osmotolerant *Escherichia coli* mutants frequently exhibit defective

- N-acetylglucosamine catabolism and point mutations in cell shape-regulating protein MreB. *Appl Environ Microbiol* 80:3729–3740
49. Pereira MF, Rossi CC, Seide LE, Martins Filho S, Dolinski CM, Bazzolli DMS (2018) Antimicrobial resistance, biofilm formation and virulence reveal *Actinobacillus pleuropneumoniae* strains' pathogenicity complexity. *Res Vet Sci* 118:498–501
 50. Archambault M, Harel J, Gouré J, Tremblay YD, Jacques M (2012) Antimicrobial susceptibilities and resistance genes of Canadian isolates of *Actinobacillus pleuropneumoniae*. *Microb Drug Resist* 18:198–206
 51. Huda N, Lee EW, Chen J, Morita Y, Kuroda T, Mizushima T, Tsuchiya T (2003) Molecular cloning and characterization of an ABC multidrug efflux pump, VcaM, in Non-O1 *Vibrio cholerae*. *Antimicrob Agents Chemother* 47:2413–2417
 52. Alav I, Kobylka J, Kuth MS, Pos KM, Picard M, Blair JMA, Bavro VN (2021) Structure, assembly, and function of tripartite efflux and type 1 secretion systems in gram-negative bacteria. *Chem Rev* 121:5479–5596
 53. Lobritz MA, Belenky P, Porter CB, Gutierrez A, Yang JH, Schwarz EG, Dwyer DJ, Khalil AS, Collins JJ (2015) Antibiotic efficacy is linked to bacterial cellular respiration. *Proc Natl Acad Sci USA* 112:8173–8180
 54. Zeng J, Hong Y, Zhao N, Liu Q, Zhu W, Xiao L, Wang W, Chen M, Hong S, Wu L, Xue Y, Wang D, Niu J, Drlica K, Zhao X (2022) A broadly applicable, stress-mediated bacterial death pathway regulated by the phosphotransferase system (PTS) and the cAMP-Crp cascade. *Proc Natl Acad Sci USA* 119:e2118566119
 55. Boekema BK, Kamp EM, Smits MA, Smith HE, Stockhofe-Zurwieden N (2004) Both ApxI and ApxII of *Actinobacillus pleuropneumoniae* serotype 1 are necessary for full virulence. *Vet Microbiol* 100:17–23
 56. Spero MA, Newman DK (2018) Chlorate specifically targets oxidant-starved, antibiotic-tolerant populations of *Pseudomonas aeruginosa* biofilms. *mBio* 9:e01400-18
 57. Buettner FF, Bendalla IM, Bossé JT, Meens J, Nash JH, Härtig E, Langford PR, Gerlach GF (2009) Analysis of the *Actinobacillus pleuropneumoniae* HlyX (FNR) regulon and identification of iron-regulated protein B as an essential virulence factor. *Proteomics* 9:2383–2398
 58. Browning DF, Cole JA, Busby SJ (2000) Suppression of FNR-dependent transcription activation at the *Escherichia coli* *nir* promoter by Fis, IHF and H-NS: modulation of transcription initiation by a complex nucleoid-protein assembly. *Mol Microbiol* 37:1258–1269
 59. Myers KS, Yan H, Ong IM, Chung D, Liang K, Tran F, Keleş S, Landick R, Kiley PJ (2013) Genome-scale analysis of *Escherichia coli* FNR reveals complex features of transcription factor binding. *PLoS Genet* 9:e1003565
 60. Gawade P, Gunjal G, Sharma A, Ghosh P (2020) Reconstruction of transcriptional regulatory networks of Fis and H-NS in *Escherichia coli* from genome-wide data analysis. *Genomics* 112:1264–1272
 61. Browning DF, Grainger DC, Beatty CM, Wolfe AJ, Cole JA, Busby SJ (2005) Integration of three signals at the *Escherichia coli* *nrf* promoter: a role for Fis protein in catabolite repression. *Mol Microbiol* 57:496–510
 62. Browning DF, Cole JA, Busby SJ (2008) Regulation by nucleoid-associated proteins at the *Escherichia coli* *nir* operon promoter. *J Bacteriol* 190:7258–7267
 63. Baker P, Hill PJ, Snarr BD, Alnabesey A, Pestrak MJ, Lee MJ, Jennings LK, Tam J, Melnyk RA, Parsek MR, Sheppard DC, Wozniak DJ, Howell PL (2016) Exopolysaccharide biosynthetic glycoside hydrolases can be utilized to disrupt and prevent *Pseudomonas aeruginosa* biofilms. *Sci Adv* 2:e1501632
 64. Goodman SD, Obergfell KP, Jurcisek JA, Novotny LA, Downey JS, Ayala EA, Tjokro N, Li B, Justice SS, Bakaletz LO (2011) Biofilms can be dispersed by focusing the immune system on a common family of bacterial nucleoid-associated proteins. *Mucosal Immunol* 4:625–637
 65. Cherny KE, Sauer K (2019) *Pseudomonas aeruginosa* requires the DNA-specific endonuclease EndA to degrade extracellular genomic DNA to disperse from the biofilm. *J Bacteriol* 201:e00059-e119
 66. Iwase T, Uehara Y, Shinji H, Tajima A, Seo H, Takada K, Agata T, Mizunoe Y (2010) *Staphylococcus epidermidis* Esp inhibits *Staphylococcus aureus* biofilm formation and nasal colonization. *Nature* 465:346–349
 67. Sambanthamoorthy K, Sloup RE, Parashar V, Smith JM, Kim EE, Semmelhack MF, Neiditch MB, Waters CM (2012) Identification of small molecules that antagonize diguanylate cyclase enzymes to inhibit biofilm formation. *Antimicrob Agents Chemother* 56:5202–5211
 68. Anderson JK, Huang JY, Wreden C, Sweeney EG, Goers J, Remington SJ, Guillemin K (2015) Chemorepulsion from the quorum signal

autoinducer-2 promotes *Helicobacter pylori* biofilm dispersal. *mBio* 6:e00379

Publisher's Note

Springer Nature remains neutral with regard to jurisdictional claims in published maps and institutional affiliations.

Ready to submit your research? Choose BMC and benefit from:

- fast, convenient online submission
- thorough peer review by experienced researchers in your field
- rapid publication on acceptance
- support for research data, including large and complex data types
- gold Open Access which fosters wider collaboration and increased citations
- maximum visibility for your research: over 100M website views per year

At BMC, research is always in progress.

Learn more biomedcentral.com/submissions

